Magnetotransport of a quasi-three-dimensional electron gas in the lowest Landau level

G. M. Gusev, A. A. Quivy, T. E. Lamas, and J. R. Leite
Instituto de Física da Universidade de São Paulo, São Paulo, Brazil

A. K. Bakarov and A. I. Toropov
Institute of Semiconductor Physics, Novosibirsk, Russia

O. Estibals
GHMF, MPI-FKF/CNRS, BP-166, F-38042, Grenoble, Cedex 9, France
and INSA-Toulouse, 31077, Cedex 4, France

J. C. Portal
GHMF, MPI-FKF/CNRS, BP-166, F-38042, Grenoble, Cedex 9, France;
INSA-Toulouse, 31077, Cedex 4, France;
and Institut Universitaire de France, Toulose, France
(Received 25 January 2002; published 13 May 2002)

We have observed features in the magnetoresistance of a wide parabolic quantum well in the presence of the in-plane magnetic field at field three times larger than fundamental field corresponding to the depopulation of the last Landau level. The magnetoresistance structures shift with a specific sample parameter, such as potential width. We suggested the formation of correlated states of a three-dimensional electron gas at Landau filling factor 1/3, in analogy with a two-dimensional fractional quantum Hall effect.

DOI: 10.1103/PhysRevB.65.205316 PACS number(s): 72.20.My, 71.45.−d, 73.21.Fg

I. INTRODUCTION

Two-dimensional electron gas in high magnetic field exhibits several novel electronic correlated phases.[1] The most remarkable example is the electronic states of the fractional quantum Hall effect (FQHE).[2] Many-body effects in low-density three-dimensional electron gas (3DEG) in the presence of a strong magnetic field have not yet been identified unambigously. It has been shown that at sufficiently low temperatures the uniform 3DEG should be unstable with respect to the formation of a spin density wave (SDW) (Ref. 3) or charge-density wave (CDW) (Ref. 4) in strong magnetic field. The reasons for the possible formation of SDW (CDW) are the one-dimensional character of the electron motion in a strong magnetic field and electron-electron interaction. The spin (charge) density wave is pinned in the crystal due to the interaction with an arbitrarily small density of impurities.[5]

The best candidate for the study of three-dimensional (3D) many-body effects in a strong magnetic field is a remotely doped wide parabolic quantum well (WPQW), because it allows to form a wide layer of dilute high mobility carriers with a uniform density.[6] In Ref. 7 a realistic WPQW has been considered and the parameters of the system as well as the temperature and magnetic-field ranges necessary for the observation of the new electronic correlated phases have been calculated. Theoretical calculations support the possibility of the observation of these effects in realistic structure, however, the spin-density wave instability is very sensitive to the choice of parameters. This probably explains why neither SDW nor CDW have been observed so far in experiments on magnetotransport in wide parabolic quantum wells.[6,8–11]

In this paper we report magnetotransport measurements in the wide slab of electrons in AlGaAs parabolic quantum well in the presence of the in-plane magnetic field B. We have observed new structures in the magnetoresistance in the quantum limit at $B_{1/3}=3B_1$, when B_1 corresponds to the depopulation of the $n=1$ Landau level (LL). Dependent on the direction of the current (i.e., parallel or perpendicular to the magnetic field) the magnetoresistance shows either a peak or a smooth step. The magnetotransport features may be indicative of a new correlated electronic state, which is formed in the extreme quantum limit at $B_{1/3}=3B_1$. The origin of this state remains unclear. More recent theories[12] treat the pure 3DEG in the Hartree-Fock approximation in the extreme quantum limit. A complicated phase diagram has been predicted for the transition region from the uniform gas state to the Wigner crystal as the magnetic field is increased,[13] however, no discontinuity in the ground-state energy near $B_{1/3}=3B_1$ was found. The situation resembles that of two-dimensional systems, where the FQHE has been discovered at Landau filling factor 1/3 demonstrating the failure of the Hartree-Fock theory. It is only recently that a new, correlated, stripe phase has been observed in the higher LL in samples with exceptionally high mobilities,[14] which is consistent with the theoretical suggestion of charge-density wave states at the levels with $n>1$. The properties of the 3D systems in the extreme quantum limit are also, probably, beyond the Hartree-Fock approximation. The transport measurements discussed in our paper may offer the way to determine the ground state in 3D system in the strong magnetic field.

II. ELECTRON STATES OF A WIDE PARABOLIC WELL IN THE PRESENCE OF THE PERPENDICULAR AND IN-PLANE MAGNETIC FIELD

The modulation doped quasi-three-dimensional structures were suggested by Gossard and Halperin[5] and were grown

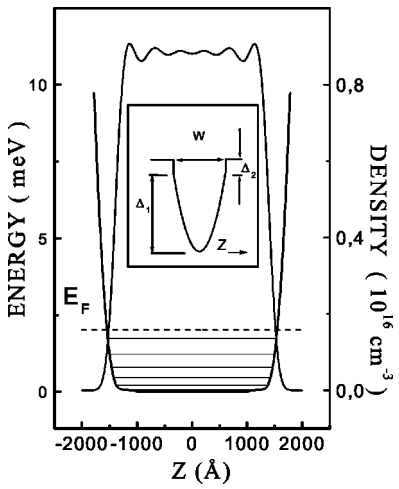

FIG. 1. Calculated total potential, electron density, and energy levels in 4000-Å parabolic quantum well for sheet density, $n_s = 2.3\times10^{11}$ cm^{-2}. Inset shows schematic illustration of the conduction-band edge in an empty parabolic well.

by Sundaram *et al.*[8] and by Shayegan *et al.*[9] It has been demonstrated that the electrons in the well occupy several (up to four) electric subbands.[6,10,11] Self-consistent calculations for a partially full 4000-Å parabolic well with the electronic slab width $W_e = 3000$ Å and the sheet density 2.3×10^{11} cm^{-2}, which are shown in Fig. 1, reveals six subbands occupied. The number of the occupied electric subbands and the effective width can be increased by increasing of the electron sheet density. We may conclude here, that the system in zero magnetic field is neither two dimensional (2D) nor three dimensional (3D). In the presence of the in-plane magnetic field, however, evolution of 2D-3D energy spectrum is expected. The energy of the electrons in a parabolic quantum well with the potential $V=(az)^2$ in the presence of an in-plane magnetic field oriented along x axis is given by

$$E_n=(\hbar^2/2m)(k_x^2+\gamma k_y^2)+\hbar\omega(n+1/2) \quad (n=0,1,\ldots), \tag{1}$$

where $\omega=(\omega_o+\omega_c)^{1/2}$, $\omega_o=a(2/m)^{1/2}$, $\omega_c=eB/m$, $\gamma=(\omega_o/\omega)^2$, and m is effective mass. For wide parabolic wells in strong magnetic field $\omega_o \ll \omega_c$, and we have

$$E_n \approx \hbar\omega_c(n+1/2)+\hbar^2k_x^2/2m, \tag{2}$$

which is the energy of the 3D LL subbands, where n is the LL number. For the square quantum well this problem cannot be solved analytically. However, one can expect that the results for both approximations in strong magnetic field would not be different. The energy spectrum in parallel magnetic field is schematically shown in Fig. 2, where the energy levels at $B=0$ are taken from our self-consistent calculations. Also dots represent the bulk Landau level. We can see that the $n=2$ and $n=1$ bulk LL's are almost coincident with subband energies in strong field. Therefore, it is expected that the physics of the wide parabolic well and 3D systems in this case should be similar. It follows from the fact that in 1 T the magnetic length is equal to 250 Å, which is 15 times

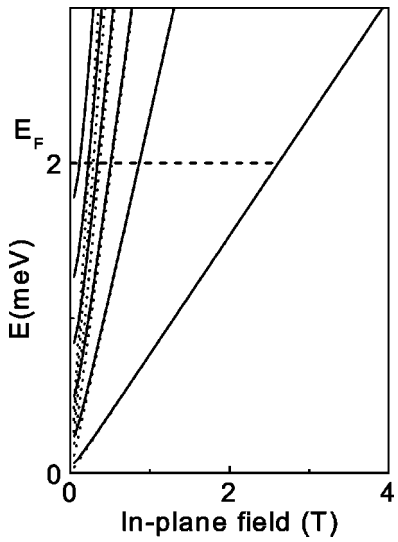

FIG. 2. Energy levels of the wide parabolic quantum well as a function of the in-plane magnetic field. Dots represents the bulk Landau levels. The position of the Fermi level at zero magnetic field is shown by the dashed line.

smaller than the width of our well, and electron system in such field is essentially three dimensional.

In a magnetic field directed along z axis each subband represents a staircase of LL associated with the subband energy E_i (i is the subband index). The energy spectrum of the electron states is given by

$$E_{in}=E_i+\hbar\omega_c(n+1/2). \tag{3}$$

Clearly, this energy spectrum is different from the energy of the 3D LL subbands in the presence of the in-plane magnetic field described by Eq. (2). It is shown schematically in Fig. 3 again for the energy levels at $B=0$ determined from self-consistent calculations. The three-dimensional limit in

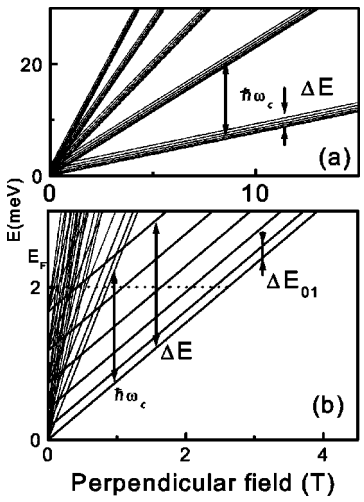

FIG. 3. Energy of the wide parabolic quantum well as a function of the strong (a) and low (b) perpendicular magnetic field. The position of the Fermi level at zero magnetic field is shown by the dashed line. The cyclotron and subband energies are indicated. Five Landau levels are shown. Spin splitting is neglected.

TABLE I. The sample parameters.

Sample	x	y	d (Å)	W (Å)	n_s (Dark) (10^{11} cm^{-2})	μ (Dark) (cm^2/Vs)	n_s (After illumination) (10^{11} cm^{-2})	μ (After illumination) (cm^2/Vs)
2236	0.275	0.275	150	2000	1.1	67000	2.8	66000
2237	0.275	0.275	150	2000	1.4	85000	3.4	61000
2262	0.200	0.310	200	1000	1	71000	5.8	108000
2263	0.270	0.310	150	1500	1.5	83000	5.6	79000
2264	0.270	0.310	150	2000	2	81000	4.5	73000
2265	0.270	0.310	150	2500	2	71000	3.8	65000
2266	0.270	0.310	150	3000	2.4	82000	4.8	61000
*AG*662	0.270	0.310	100	4000	1.5	120000	3.5	240000

this geometry may be reached by continuously increasing the width of the parabolic well, when the distance between levels $\Delta E_{ij} \rightarrow 0$. In a real system the energy levels have a finite width due to the disorder Γ, therefore, the electron system has a 3D energy spectrum when the electron subbands and their LL overlap, $\Gamma \sim \Delta E_{ij}$. We can also see clear difference between these two geometries: when the parallel magnetic field is applied, 2D-3D transition occurs in the strong enough magnetic field, in contrast to perpendicular field geometry, when magnetic field cannot change the dimensionality of the system. Based on these arguments, further we present the results of the measurements of the wide parabolic well in the presence of the strong in-plane magnetic field, when the energy spectrum is identical to the spectrum of the bulk systems.

III. CHARACTERIZATION OF THE SAMPLES AND EXPERIMENTAL DETAILS

The samples were made from $Al_xGa_{1-x}As$ parabolic quantum well grown by molecular-beam epitaxy. It included a 4000 Å-wide parabolic $Al_xGa_{x-1}As$ well with x varying between 0 and 0.29, bounded by undoped $Al_yGa_{y-1}As$ spacer layers with δ-Si doping on two sides. The thickness d of the undoped layer was 100–200 Å. The well is characterized by three parameters shown in the inset to Fig. 1. The height of the parabola $\Delta_1 = 750x$ meV, the width of the parabola W, and the height of the AlGaAs barrier $\Delta_2 = 750(y - x)$ meV. The parabolic variations mimic the potential of a uniform positive three-dimensional charge n^+, which is proportional to the curvature of the grown parabolic potential. The parabolic well is full, when the electron sheet density in the well n_s is sufficient to completely screen the fictitious positive charge n^+: $n_s = n^+ W = 2\Delta_1 \varepsilon / (e^2 \pi W)$, where $\varepsilon = 12.87$ is the static dielectric constant. The sample parameters are given in the Table I. Initially all our parabolic wells are only partially occupied by electrons. We varied the electron sheet density by illumination with a red light-emitting diode. In order to increase the full well sheet density with respect to the previously studied WPQW,[6,11] we increased the height of the parabola for several structures (see Table I). The mobility of the electron gas in our samples varies from 60×10^3 cm^2/Vs for 1000–3000 Å parabolic wells to 210×10^3 cm^2/Vs for a 4000-Å well. It should be noted, that the mobility in a WPQW is usually smaller than in the conventional AlGaAs structures due to such scattering mechanisms as background impurity and alloy disorder scattering. The mobility due to the remote and background impurity scattering in our structures has been calculated in paper Ref. 15. We found that the remote impurity scattering has no a strong effect in a wide well, since the distance between the impurities and the edge of the electron slab is larger than the spacer width. On the other hand, the role of the background impurities increases dramatically in comparison with conventional GaAs/AlGaAs heterostructures. For homogeneous background doping the scattering time τ is given by[16]

$$\hbar/\tau = (2E_F N_B W/n_s) H(k_F), \tag{4}$$

where E_F is the Fermi energy, N_B is background doping density, and $H(k_F)$ is the screening function that depends on the Fermi vector k_F. In Ref. 17 it was argued that in heterostructures with high mobility the major scattering mechanism is due to the background doping. For heterostructures the Eq. (4) can be rewritten in the form $\hbar/\tau = E_F N_B / n_s k_F$. This expression gives the mobility in 2D electron gas $\mu_{2D} = 5 \times 10^6$ cm^2/Vs for $n_s = 3 \times 10^{11}$ cm^{-2} and $N_B = 1.1 \times 10^{14}$ cm^{-3}, which is close to the limit of the expected carbon impurity contamination in the well.[17] Therefore, from the comparison of the mobility in the wide well μ_{well} and in heterostructures μ_{2D} we obtain $\mu_{well} = 2\mu_{2D}/(Wk_F) \approx 180 \times 10^3$ cm^2/Vs, which is close to the experimental value of the mobility for our 4000-Å parabolic well with the same electron sheet density. Thus, we may conclude here that the quality of our best samples is comparable with the GaAs/AlGaAs heterostructures containing 2D electron gas with mobility $\mu_{2D} > 5 \times 10^6$ cm^2/Vs.

The test samples were Hall bars with the distance between the voltage probes $L = 200$ μm and the width of the bar $d = 100$ μm. Four-terminal resistance and Hall measurements were made down to 50 mK in a magnetic field up to 15 T. The sample was immersed in a mixing chamber of a top-loading dilution refrigerator. The measurements were performed with an ac current not exceeding 10^{-7} A. Resistance

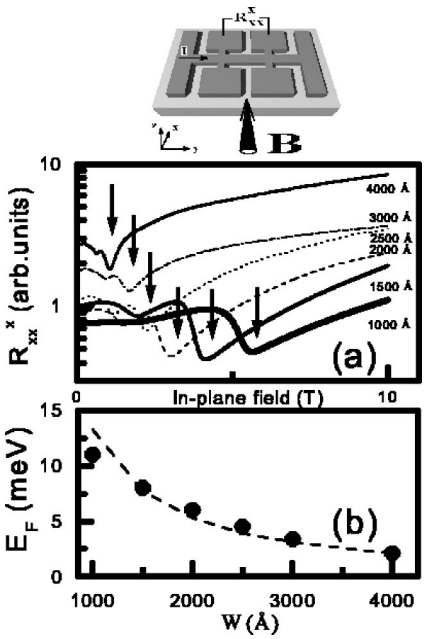

FIG. 4. (*Top*) Sketch of the experimental geometry for the measurements of the transverse magnetoresistance R_{xx}^x. (a) R_{xx}^x as a function of the in-plane magnetic field for wells with different geometrical widths W, $T=1.5$ K. Curves are shifted for clarity. Arrows show the position of the fundamental magnetic field B_1 corresponding to the depopulation of the last Landau level. (b) Fermi energy of the quasi-three-dimensional electron gas as a function of the sample width extracted from the position of the last magnetoresistance minima. Dashes represent data of Eq. (5).

was measured for different angles between the field, substrate plane, and current in magnetic field using an *in situ* rotation of the sample. The current was directed along the Hall bar (y axis). We measured the longitudinal magnetoresistance R_{yy} with magnetic field directed along y axis, and the transverse magnetoresistance R_{xx}^x with B oriented perpendicular to the current (x axis) and parallel to the quantum well. R_{xx}^z denotes transverse magnetoresistance when magnetic field is directed parallel to the normal of the quantum well plane (z axis). We rotate the sample *in situ*, so that magnetic field could be tilted with respect to the sample (x-y) plane in x or in y directions. We denote the angle between B and the sample plane by Θ. We used the Hall voltage for the measurements of the tilt angle with precision of 0.02°. We investigated 1–3 samples with similar parameters for each grown structure indicated in the Table I. The concentration was determined from the low-field Hall measurements. In addition to the Hall bar we performed measurements in the van der Paw structures.

IV. EXPERIMENTAL RESULTS

Figure 4(a) shows the transverse resistance R_{xx}^x as a function of in-plane magnetic field for parabolic wells with different geometric widths at $T=1.5$ K. As we already mention in the Sec. II, in parabolic quantum well the subband energy is determined by Eq. (1) (see also Fig. 2), and the magnetoresistance reveals oscillations, sometimes called diamagnetic Shubnikov de-Haas (SdH) oscillations, which result from the combined effect of the electric and magnetic fields.[18] In quantum well with several subbands occupied, such oscillations can be interpreted as magnetic depopulation of the 2D levels. However, as we also discussed above, the energies of the $i=1$ and $i=0$ subbands in magnetic field are coincident with the energy of the $n=1$ and $n=0$ bulk Landau levels, therefore, last oscillations correspond to the depopulation of the bulk LL. To distinguish between these two cases we should consider characteristic energy of the quantum well $E_0=(2\pi)^2\hbar^2/(8mW^2)$ and cyclotron energy $\hbar\omega_c$, which for the last magnetoresistance minima is equal to Fermi energy. For full parabolic well we have

$$E_F=\hbar^2(3\pi^2N_+)^{2/3}/(2mW^{4/3}), \tag{5}$$

where $N_+=n_+W^2$. Since $E_0\sim W^{-2}$ and $E_F\sim W^{-4/3}$ we may estimate critical width $W_c\sim 100$ Å, when $E_0\sim E_F$. For wider parabolic wells, $E_0\ll E_F$, and the energy of the $n=0$ bulk LL level is coincident with the energy of $i=0$ subband. Figure 4(b) shows the Fermi energy determined from the position of the last minimum of the magnetoresistance and fit of the Eq. (5) without adjustable parameters. It is worth to note that in contrast to 2D electron gas in conventional GaAs/AlGaAs structures, we cannot change the bulk Fermi energy in parabolic well by increasing the electron sheet density through illumination. It results from the fact that the width of the electron slab W_e increases with n_s, so that the bulk density $n_{bulk}=n_s/W_e$ and the Fermi energy remain essentially constant. Indeed we cannot fill up the parabolic well with density $n_{bulk}>n_+$, since the electrons in the wide well due to the electrostatic repulsion will be separated into two weakly connected two-dimensional systems. Therefore, the only way to vary Fermi energy is the variation of the geometrical width of the parabolic well. It introduces some limits for the investigation of the 3D properties in such systems. For example, it would be better to increase the width of the well to improve 3D approximation, specially for perpendicular magnetic field. However, as we can see in Fig. 4(b), the Fermi energy decreases rapidly and all magnetic energy scales shift to the lower fields. Because of these natural limitations, we believe that the 4000 Å parabolic wells are, probably, optimal systems for investigation of correlation effects in 3D gas. Figure 5 gives additional support for this assumption. It represents the low-field part of the magnetoresistance of the 4000-Å well at low temperature $T=50$ mK. We can see magnetoresistance oscillations at low field and the fit of the theoretical expression for 3D SdH (Ref. 20) to the experimental curve assuming parameters $E_F=2.04$ meV and the single-particle relaxation time $\tau_s\approx 10^{-12}$ s. One may see that the periodicity of the first oscillation deviates from $1/B$ behavior, which results from the combined effect of the electric and magnetic fields. The resistivity minimum in 3D case produced by the depopulation of the nth LL occurs at the inverse magnetic field given by[20]

$$B_n^{-1}=P(n+1/8+\beta), \tag{6}$$

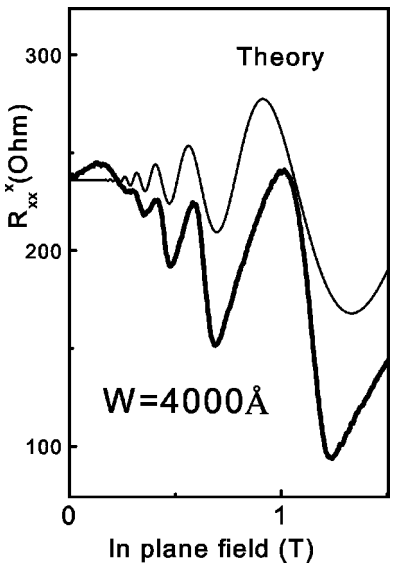

FIG. 5. Transverse magnetoresistance R_{xx}^{x} as a function of the low in-plane magnetic field for parabolic well with geometrical width $W=4000$ Å, $T=50$ mK. Thin line represents SdH oscillations in 3D case calculated from theoretical expression (see, for example, Ref. 20).

where for the spherical model $P=(2e/\hbar)(3\pi^2 n_{bulk})^{-2/3}$, $\beta=0.5$. From Eq. (6) we find that the last minimum at $B_1=1.1$ T corresponds to the depopulation of the $n=1$ Landau level, and at higher fields only the lowest LL is occupied.

Now we turn to the experimental results in the quantum limits in the strong in-plane magnetic field. Figure 6 shows the transverse resistance R_{xx}^{x} as a function of in-plane magnetic field for different electron sheet densities for 4000-Å parabolic well. Surprisingly, at $B=3.7T\approx 3B_1$ (LL number $n=1/3$), we observe a peak in the transverse magnetoresistance, as can be seen in Fig. 6. This peak becomes sharper with the increase of the electron density [Fig. 6(a)]. Figure 6(b) shows the data for the second sample, when after illumination we approach a slightly higher Fermi energy. We can see that both the last Landau minimum and the peak at higher magnetic field are shifted to lower magnetic fields. The feature at three times the fundamental depopulation field is comparable with the SdH oscillations, and it seems to be strong. Its precise position in magnetic field should depend on the Fermi energy and sample design.

In order to observed the feature shift with a specific sample parameter we study the samples with smaller widths. Figure 7 shows the experimental traces of R_{xx}^{x} from four samples taken at different temperatures. We can see that the data from all samples show the peak at $B_{1/3}=3B_1$. As temperature is raised above 0.5–1 K the 1/3 feature is gradually vanishing. The feature depends on the mobility and is weaker in samples with lower mobilities. Because samples with widths 2000–3000 Å have similar mobilities, it seems that the feature becomes weaker for lower magnetic fields. This data, probably, explains why samples with similar design investigated in Ref. 19 did not reveal structures observed in our work, the mobility of the sample was 50×10^3 cm^2/Vs, which is marginal for the observation of the 1/3 structures

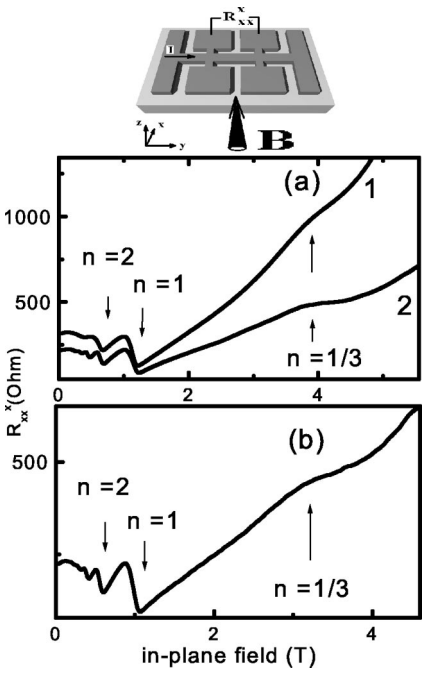

FIG. 6. (*Top*) Sketch of the experimental geometry for the measurements of the transverse magnetoresistance R_{xx}^{x}. (a) Sample 1; R_{xx}^{x} as a function of the in-plane magnetic field for two different values of the density n_s: 1.5×10^{11} cm^{-2} (curve 1) and 3.5×10^{11} cm^{-2} (curve 2), $T=50$ mK. (b) Sample 2 ($n_s=3.3\times 10^{11}$ cm^{-2}), R_{xx}^{x} as a function of the in-plane magnetic field at $T=50$ mK.

[see Fig. 6(a)]. Figure 8 shows a summary of the positions of the minima in R_{xx}^{x} and 1/3 feature. Solid lines are linear dependences $1/n$ on the in-plane field, which are drawn through $n=1$ minima.

Naively, one would expect to see a spin splitting of the SdH oscillations, which would lead to the last resistivity minimum at $B\approx 2.2$–2.4 T, corresponding to the depopulation of one spin-split sublevel of the last LL.[20] However, the effective mass and the effective g factor in GaAs are such that the Zeeman splitting is roughly 1/60 of the LL spacing. In $Al_xGa_{x-1}As$, g factor increases monotonically

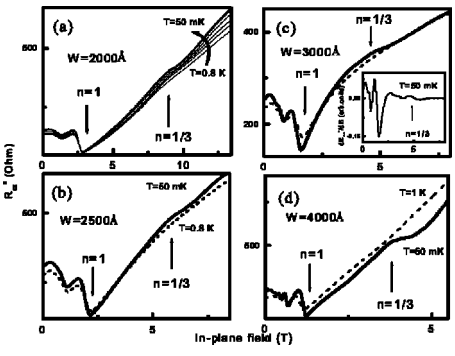

FIG. 7. Transverse magnetoresistance R_{xx}^{x} as a function of the in-plane magnetic field for parabolic wells with various widths for different temperatures: dashes represent 1.0 K, thick line represent 50 mK. Inset to (c) represents derivative of R_{xx}^{x} as a function of the in-plane magnetic field at $T=50$ mK.

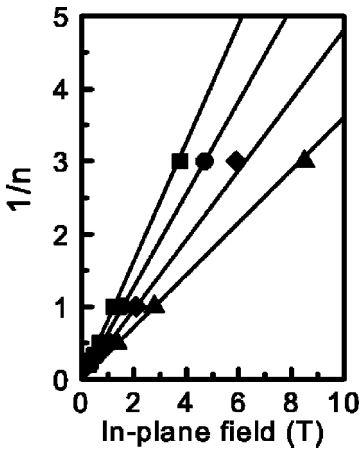

FIG. 8. Plot of the in-plane field position of the minima in transverse magnetoresistance R_{xx}^{x} corresponding to the depopulation of the nth Landau level and maxima at 1/3 feature versus $1/n$ for parabolic wells with different geometrical widths: squares represent $W=4000$ Å, circles represent $W=3000$ Å, diamonds represent $W=2500$ Å, and triangles represent $W=2000$ Å.

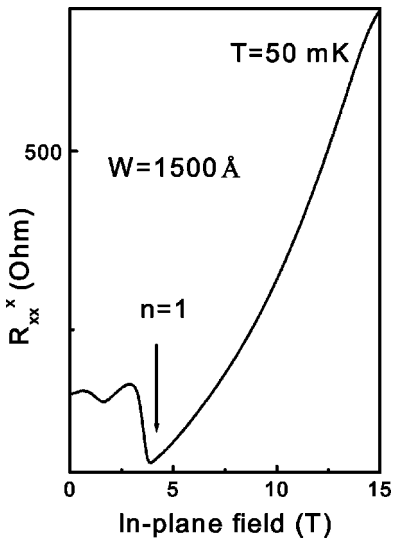

FIG. 9. Transverse magnetoresistance R_{xx}^{x} as a function of the in-plane magnetic field for a parabolic well with geometrical width $W=1500$ Å, $n_s=3.5\times10^{11}$ cm^{-2}, $T=50$ mK.

from $g=-0.44$ at $x=0$ (GaAs) to $g\approx+0.5$ at $x=0.35$ vanishing at $x\simeq0.13$.[21] It leads to the average g factor in our 4000-Å parabolic well of 0.14 and corresponding Zeeman energy $\Delta E_Z=0.02$ meV at $B=2.4$ T. It is worth mentioning that the possibility of the observation of spin-split instead of single peaks depends not only on their separation and temperature, but also on the level broadening. Collapse of the spin splitting can be interpreted as a result of the overlapping of LL subbands, when level broadening Γ is larger than the Zeeman energy. The width of the LL is determined by the single-particle relaxation time τ_s, which is usually smaller than the transport time obtained from the conductivity at $B=0$. As we indicated above, from the comparison of the SdH oscillations with the conventional expression for 3D SdH effects[20] we obtained the single-particle relaxation time $\tau_s\approx10^{-12}$ s, which corresponds to the Landau level broadening $\Gamma\simeq\hbar/\tau_s\sim0.6$ meV$\gg\Delta E_Z$, supporting the arguments about the absence of spin splitting in our parabolic wells. Therefore, it can be expected that the last LL remains unpolarized in magnetic fields up to $\simeq50$ T, when $\Gamma\simeq\Delta E_Z$. Indeed, in the true $B\rightarrow\infty$ limit the Zeeman splitting would maximally polarize the system, however, no resistivity minima should be observed in this case. In two-dimensional systems g factor is strongly enhanced due to the electron-electron correlation effects, therefore, in 2DEG it is easy to approach extreme quantum limit, when only the lower spin state of the lowest Landau levels are occupied.

Indeed we extended our measurements to higher fields up to 15 T in order to look for the occurrence of similar phenomena at other fractional fillings like 1/5. We found that in the quantum limit R_{xx}^{x} exhibits linear dependence on the magnetic field with a larger slope for the transverse magnetoresistance and a weak temperature dependence in the liquid-helium range (1–4.2 K). At low temperatures magnetoresistance demonstrates a stronger magnetic-field dependence at $B>7$ T, which may be indicative of the beginning of the magnetic freeze-out, however, no indication for other fractional features at higher magnetic field was found. It is not very surprising, since the mobility in our samples is low, in comparison with 2D electron gas. As has been demonstrated in Ref. 22, the samples with 2D mobility smaller than 500×10^{3} cm^2/Vs reveal transition to the insulating states after 1/3 minimum without development of the 1/5 and other high-order fractional features.

Figure 9 shows the transverse resistance R_{xx}^{x} as a function of in-plane magnetic field for 1500-Å parabolic well. Since the last minimum occurs at $B_1\approx4$ T, we expected that the 1/3 features will appear at $B_{1/3}\approx12$ T. However, no feature at this field was found. It is not very surprising too, and we may argue here that the stronger magnetic field kills the 1/3 feature due to competitions between one-dimensional localization and correlation effects.[23] The transition to the insulating state in 2D samples,[22] mentioned above supports this idea. Higher mobility samples are necessary to check the influence of the strong magnetic-field localization on the correlation effects.

We also measured magnetoresistance in 1000-Å parabolic well, when 1/3 feature is expected to be close to 18 T. Since our measurements are limited to 15 T, we looked for 2/3 or other fractional features at lower fields. These features were nor observed in our samples.

To finish the part of work concerning the measurements in a parallel magnetic field, we have to mention another experimental geometry. We have also measured the longitudinal resistivity R_{yy} (the current in parallel with B) as a function of the in-plane magnetic field. For comparison we show the data for both configurations in Fig. 10. Surprisingly, the magnetoresistance exhibits anisotropic behavior; we see the peak in R_{xx}^{x} accompanied by the changes in the slope of R_{yy} (step) roughly centered at $n=1/3$. At $T=1.5$ K the curves exhibit only a monotonic increase with magnetic field, as can be seen in Fig. 11. In Fig. 10 we can see that the SdH oscillations in the longitudinal magnetoresistance have a smaller amplitude and are shifted to lower field. For the transverse

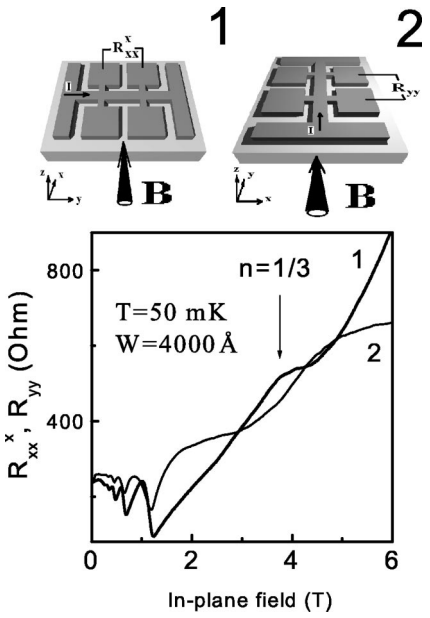

FIG. 10. (*Top*) Sketch of the experimental geometry for the measurements of the transverse R_{xx}^x and longitudinal R_{yy} magnetoresistance. R_{xx}^x (1) and R_{yy} (2) as a function of in-plane magnetic field for a parabolic well with geometrical width $W=4000$ Å, $n_s=3.5\times10^{11}$ cm^{-2}, and $T=50$ mK.

SdH oscillations the theory predicts the amplitude, a factor 2.5 times larger than that for R_{yy}, which is roughly consistent with our measurements. However, the shift of the peaks remains unclear. It should be noted that a similar shift for diamagnetic SdH oscillations has been observed in narrow

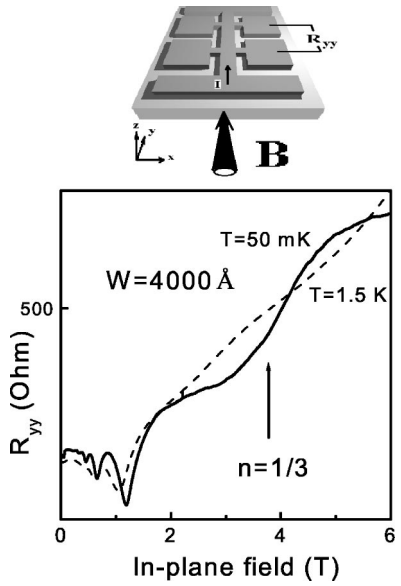

FIG. 11. (*Top*) Sketch of the experimental geometry for the measurements of the longitudinal magnetoresistance R_{yy}. R_{yy} as a function of the in-plane magnetic field for a parabolic well with geometrical width $W=4000$ Å for different temperatures: dashes represent $T=1.5$ K, thick line represent $T=50$ mK, and $n_s=1.5\times10^{11}$ cm^{-2}.

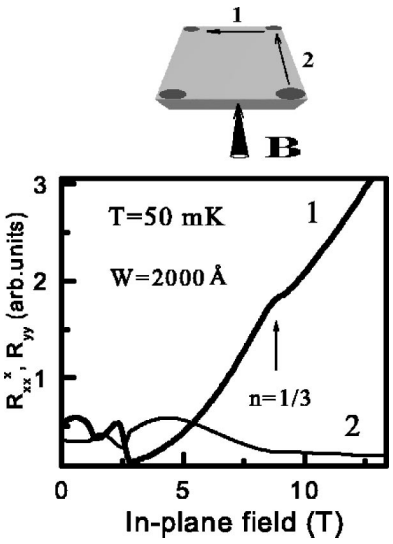

FIG. 12. (*Top*) Van der Paw geometry for the measurements of the longitudinal and transverse magnetoresistance; arrows show the direction of the current. R_{xx} (1) and R_{yy} (2) as a function of the in-plane magnetic field for a parabolic well with geometrical width $W=2000$ Å at $T=50$ mK, $n_s=2.1\times10^{11}$ cm^{-2}.

parabolic quantum well.[18] In the quantum limit R_{xx}^x and R_{yy} both exhibit linear dependence on the magnetic field with a larger slope for the transverse magnetoresistance at $T=1.5$ K. We have to note that anisotropic behavior of magnetoresistance in the quantum limit for ionized impurity case without correlation effects has been predicted and observed in a number of 3D systems (for review see Ref. 23). Here we report on the anisotropy close to the magnetic field $B_{1/3}$. We emphasize that not only $R_{xx}^x \gg R_{yy}$, but 1/3 features have a different shape for these geometries.

In 2D electron gas it has been shown that the influence of anisotropy in transport can be dramatically enhanced by use of a van der Paw geometry.[24] We also measured longitudinal and transverse magnetoresistances in the parallel magnetic field for this geometry, shown in Fig. 12. Indeed 1/3 features are observed in van der Paw sample, where R_{xx}^x reveals the peak at $B_{1/3}=3B_1$ and increases at $B>B_1$. Behavior of the longitudinal magnetoresistance was found to be different from the dependence of R_{yy} on the parallel magnetic field in Hall bar geometry: R_{yy} decreases at high field and changes the slope near $B_{1/3}=3B_1$. We have to note that the nonuniform current distribution in van der Paw geometry leads to mixture between different components of the resistance, and such measurements will be very difficult to analyze, however, in this work we do not attempt to describe how magnetoresistance behaves in Hall bar and in van der Paw geometry.

As we already mention in Sec. I, energy spectrum shown in Fig. 3 transforms to the spectrum in Fig. 2, when magnetic field is tilted away from the normal to the sample plane. Evolution of the energy levels in the tilted field in parabolic quantum well has been studied in Ref. 9 for 1000-Å parabolic well. As has been argued in Ref. 9, the states in tilted field, so called oblique states, transform into plane waves

along the field in the bulk Landau states, since their localization length W_x grows as $W_x/\tan\Theta$, when field is tilted in the x direction. We also measured the resistance at different angles Θ between the field and the parabolic well plane, rotating our sample in situ. Since the degeneracy of the oblique states is given by $(eB/h)\sin\Theta$, as for 2D levels, in titled field we observe SdH oscillations shifted, as expected with the angle, similar to results, observed in Ref. 9. Previous experiments in parabolic well with the width of the electron slab $W_e \approx 1000$ Å and four occupied subbands demonstrated a 2D character of the spectrum in perpendicular magnetic field.[9,11] Our samples are wider, but it is not wide enough for the 2D-3D transition at $B=0$, and the density of states in a perpendicular magnetic field does not lose its 2D structure.[15] Due to this, the $n=1/3$ structure disappears at $\Theta > 20°$, and we observe only 2D SdH oscillations in tilted and perpendicular magnetic field at $B > 1.2$ T.

V. POSSIBLE STATES FOR THREE-DIMENSIONAL ELECTRON GAS IN THE QUANTUM LIMIT IN THE STRONG MAGNETIC FIELD

There is no satisfactory explanation for the observed magnetoresistance features near $B_{1/3}=3B_1$. It cannot be a spin-splitting effect because of a small value of the g factor and inconsistency with the behavior of conventional spin-split oscillations. Since the samples have a high electron mobility we can suggest, in analogy with a 2D FQHE, a formation of correlated electronic state. The Hartree-Fock approximation predicts several electronic phases in a strong magnetic field in the extreme quantum limit.[13] First, it has been shown that a homogeneous 3DEG should be transformed into a two-dimensional hexagonal lattice of charged rods parallel to the magnetic field with the diameter $2l_H$, where l_H is the magnetic length (Kaplan-Glasser phase).[12] Each charged rod behaves as a one-dimensional electron gas with a variation of the charge described by the wave vector $Q_y=2k_F$ along each rod, where k_F is the Fermi vector of the electrons. In our parabolic well the dimensionless interelectron spacing $r_s=(4\pi n^+/3)^{-1/3}a_B^{-1}$, where a_B is the effective Bohr radius, is around 3. According to Ref. 13, in such a situation 1D charged rods evolve continuously into a Wigner crystal as the field is increased, and transition to the Kaplan-Glasser phase does not occur. Using the results of the calculations[13] we can estimate the values of the magnetic field, when the different phase transition should occur for our 4000-Å parabolic well. The ground state changes from uniform-density states to a CDW state with wave vector parallel to the field at $B_c \approx 1.8$ T, to an uniform-density state at $B_c \approx 5$ T, and then to a Wigner crystal with the holes and electrons at $B_c \approx 5.1$ T and 9 T consequently. We may see that all these critical fields disagree with magnetic field $B_{1/3} \approx 3.7$ T, when the structures in magnetoresistance are observed. The discovery of the FQHE demonstrates that the ground state may be different from the states predicted by the Hartree-Fock approximation. In 2D systems the fractional states corresponding to the Landau filling factor $\nu=n_s 2\pi l_H^2=q/p$, where p and q are integer numbers (q is odd), have a minimum energy. For noninteracting systems the last 3D Landau level has a filling factor $\nu=2n^+\pi^2 l_H^2/k_F=1$ (neglecting spin), and k_F decreases with B. For interacting system the $\nu=1$ state is not necessarily the minimum energy state, because of the competition between the kinetic and Coulomb energy. One may speculate that $\nu=1/3$ and $k_F(B_{1/3})=k_F(0)$ state has a minimum energy and is a kind of the charge-density wave. This new state can be pinned by impurities. We cannot explain the anisotropy of the magnetoresistance structure, however, since the energy, which is necessary to move pinned charged electronic rods in the direction along the rods or in perpendicular direction is different, it certainly should lead to anisotropy of the transport coefficients. Our observation is perhaps the indication that correlation phenomena in 3D systems in strong magnetic field are quite similar to those in the lowest 2D Landau level.

VI. CONCLUSIONS

We have measured transport properties of the parabolic quantum wells with different widths subjected to in-plane magnetic field at temperatures down to 50 mK. In spite of the fact that this system is neither 2D nor 3D at zero magnetic field, when the strong parallel magnetic field is applied, the spectrum becomes identical to that of a 3D electron gas. Since the mobility in parabolic well is much higher than in the heavily doped semiconductors, such system is very promising for studying the electron correlation effect in the strong magnetic field. Another advantage is isotropic Fermi surface and single carrier type, in contrast to semimetal, like graphite and bismuth, when highly anisotropic Fermi surface and coexistence of the electrons and holes does not allow us to unambigously interpretate magnetoresistance data in the strong magnetic field. In all our samples with widths $W > 1500$ Å we observed unexpected structure at magnetic field three times larger than the fundamental field. These structures are observed only in high mobility samples and at low temperature $T < 1$ K. Several theoretical models indeed support the idea that the correlation effects in pure 3D system become very important in the quantum limit and may drive the system to the strongly correlated state. However, such models are based on the Hatree-Fock approximation, that is failed for 2D system and does not predict fractional quantum Hall effect. Therefore, we suggested that the correlated state may occur in 3D system at filling factor 1/3, in analogy with FQHE. Indeed this idea demands further theoretical and experimental confirmation.

ACKNOWLEDGMENTS

We thank Z. D. Kvon and E. B. Olshanetskii for discussions, C. S. Sergio and A. A. Bykov for assistance with the sample preparation, D. K. Maude for help with dilution refrigerator. Support of this work by FAPESP, CNPq (Brazilian agencies), USP-COFECUB, and RFFI (Contract No. 01-02-16892) is acknowledged.

[1] *Perspectives in Quantum Hall Effects*, edited by S. Das Sarma and A. Pinzuk (Wiley, New York, 1997).
[2] D.C. Tsui, H.L. Stormer, and A.C. Gossard, Phys. Rev. Lett. **48**, 1559 (1982).
[3] V. Celli and N.D. Mermin, Phys. Rev. **140**, A839 (1965).
[4] H. Fukuyama, Solid State Commun. **26**, 783 (1978).
[5] B.I. Halperin, Jpn. J. Appl. Phys., Suppl. **26**, 1913 (1987).
[6] M. Shayegan, T. Sojoto, J. Jo, M. Santos, and L. Engel, Surf. Sci. **229**, 83 (1990).
[7] L. Brey and B.I. Halperin, Phys. Rev. B **40**, 11 634 (1989).
[8] M. Sundaram, A.C. Gossard, J.H. English, and R.M. Westervelt, Superlattices Microstruct. **4**, 683 (1988).
[9] M. Shayegan, T. Sajoto, M. Santos, and C. Silvestre, Appl. Phys. Lett. **53**, 791 (1988).
[10] T. Sajoto, J. Jo, H.P. Wei, M. Santos, and M. Shayegan, J. Vac. Sci. Technol. B **7**, 311 (1989).
[11] T. Sajoto, J. Jo, L. Engel, M. Santos, and M. Shayegan, Phys. Rev. B **39**, 10 464 (1989).
[12] J.I. Kaplan and M.L. Glasser, Phys. Rev. Lett. **28**, 1077 (1972).
[13] A.H. MacDonald and G.W. Bryant, Phys. Rev. Lett. **58**, 515 (1987).
[14] M.P. Lilly, K.B. Cooper, J.P. Eisenstein, L.N. Pfeiffer, and K.W. West, Phys. Rev. Lett. **82**, 394 (1999); W. Pan, R.R. Du, H.L. Stormer, D.C. Tsui, L.N. Pfeiffer, K.W. Baldwin, and K.W. West, *ibid.* **83**, 820 (1999).
[15] C.S. Sergio, G.M. Gusev, J.R. Leite, E.B. Olshanetskii, A.A. Bykov, N.T. Moshegov, A.K. Bakarov, A.I. Toropov, D.K. Maude, O. Estibals, and J.C. Portal, Phys. Rev. B **64**, 115314 (2001).
[16] A. Gold, Phys. Rev. B **38**, 10 798 (1988).
[17] A. Gold, Appl. Phys. Lett. **54**, 2100 (1989).
[18] K. Ensslin, A. Wixforth, M. Sundaram, P.F. Hopkins, J.H. English, and A.C. Gossard, Phys. Rev. B **47**, 1366 (1993).
[19] E.G. Gwinn, R.M. Westervelt, P.F. Hopkins, A.J. Rimberg, M. Sundaram, and A.C. Gossard, Phys. Rev. B **39**, 6260 (1989).
[20] *Landau Level Spectroscopy*, edited by G. Landwehr and E.I. Rashba (Elsevier Science, Amsterdam, 1991) p. 1040.
[21] C. Weisbuch and C. Hermann, Phys. Rev. B **15**, 816 (1977).
[22] D. Shahar, D.C. Tsui, M. Shayegan, R.N. Bhatt, and J.E. Cunningham, Phys. Rev. Lett. **74**, 4511 (1995).
[23] S.S. Murzin, Phys. Usp. **43**, 349 (2000).
[24] S.H. Simon, Phys. Rev. Lett. **83**, 4223 (1999).